Direct sampling of the Susskind-Glogower phase distributions

M. Dakna, L. Knöll, and D.-G. Welsch
Friedrich-Schiller-Universität Jena, Theoretisch-Physikalisches Institut, Max-Wien-Platz 1, 07743 Jena, Germany
(Received 17 July 1996; revised manuscript received 30 October 1996)

Coarse-grained phase distributions are introduced that approximate to the Susskind-Glogower cosine and sine phase distributions to any desired degree of accuracy. The integral relations between the phase distributions and the phase-parametrized field-strength distributions observable in balanced homodyning are derived and the integral kernels are analyzed. It is shown that the phase distributions can be directly sampled from the field-strength distributions which offers the possibility of measuring the Susskind-Glogower cosine and sine phase distributions with sufficiently high precision. Numerical simulations are performed to demonstrate the applicability of the method. [S1050-2947(97)08402-3]

PACS number(s): 42.50.Dv, 03.65.Bz

I. INTRODUCTION

Although the problem of defining and measuring quantum-mechanical phases of radiation-field modes has been discussed for a long time, there has been no unified approach to the phase problem so far [1]. The reason is that there is no ''good'' (i.e., self-adjoint) phase operator in the Hilbert space. The difficulties obviously arise from the boundedness of the eigenvalue spectrum of the photon-number operator, which is the canonical conjugate of the phase operator.

One way to overcome the difficulties was proposed by Susskind and Glogower [2] who used the non-Hermitian exponential phase operator and its adjoint in order to define two Hermitian operators. From the analogy between them and classical trigonometric functions the two operators are also referred to as cosine and sine phase operators. In particular in the classical limit they exactly correspond to the cosine and the sine of the phase. Since the cosine and sine phase operators are self-adjoint, their eigenstates can be used to define proper probability distributions for observing the cosine and sine phases. However, these distributions cannot be measured, in general, simultaneously and therefore do not uniquely characterize the phase of the quantum state of a mode. This is obviously the price to pay for introducing self-adjoint operators and keeping the concept of quantum-mechanical probabilities.

In the classical limit the difference between the cosine and sine phase distributions vanishes. In particular, in classical optics the phase difference between two radiation-field modes can always be determined by simultaneously measuring the cosine and sine of the phase difference in interference experiments. Inspired by such kinds of measurements, operational approaches to the cosine and sine phase operators have also been introduced [3]. As expected, for classical fields the corresponding phase distributions agree with the quantum-mechanical Susskind-Glogower (SG) phase distributions, but for quantum fields they may be quite different from each other.

A powerful interferometric method for determining phase-sensitive properties of optical fields has been balanced homodyne detection. It is well known that from the data recorded in a succession of measurements the quantum state of a signal mode can be obtained, as was first demonstrated experimentally by Smithey, Beck, Faridani, and Raymer using optical homodyne tomography [4]. In the experiments reported in Refs. [4] and [5] the Wigner function of a single-mode squeezed vacuum is reconstructed from the measured quadrature-component histograms by convolving them with an appropriately chosen filter function (filtered backprojection) and performing the inverse Radon transform. To avoid smoothing the measured data and to improve the tomographic method, direct sampling of the density matrix has been suggested [6], and it has been demonstrated experimentally that the single-mode density matrix in the Fock basis can directly be sampled from the measured data [7]. Other advantages of the direct sampling method over inverse Radon methods are that the quantum state reconstruction and error estimation are very fast and can be performed in *real time*, so that it is no longer necessary to store large amounts of data. In particular, systematic errors can easily be reduced to any desired level of accuracy and the remaining statistical errors only reflect the finite number of measurement events. Applying direct sampling, the photon statistics of optical pulses have been time resolved with subpicosecond sampling time, two orders of magnitude better than possible with conventional methods [8]. Further, proposals have been made to extend the direct sampling method to two-mode quantum state reconstruction and the determination of internal quantum correlations of optical fields [9,10]. Recently, experiments have been performed to demonstrate the novel possibilities and determine the two-time photon-number correlations of an optical field on ultrafast time scales [10].

In this paper we show that the direct sampling method can also advantageously be used for measuring the single-mode quantum phase statistics, such as the SG quantum phase distributions, which enables one to avoid the detour via the Wigner function in Ref. [11]. In this way, the mentioned drawbacks of the Wigner-function reconstruction can be circumvented and a more direct approach to phase measurement is possible [12]. In principle, one could also try to calculate the phase distributions from the sampled density matrix in the Fock basis. Since phase and photon number can be regarded, in a sense, as complementary variables, the density matrix must be measured with very high precision to obtain the phase statistics sufficiently well. Since with in-

creasing photon number the sampling functions for the density-matrix elements are highly oscillating functions, the statistical errors drastically increase, and hence the number of measurements must substantially be increased in order to compensate for the errors. As we will see, this difficulty does not appear when the phase distributions are directly sampled from the quadrature component distributions.

Here the difficulty is that the SG cosine and sine phase states (similar to the quadrature component states) are continuous quantum states normalized to δ functions and the sampling functions needed cannot be given explicitly, but they can only be defined by some limiting process. Since in practice the precision (resolution) with which a continuous quantity can be measured is always finite, we can approach the problem of direct sampling of the SG phase distributions introducing parametrized cosine and sine phase distributions that are defined on the basis of appropriately coarse-grained SG cosine and sine phase states, which tend to the exact states when the coarse-graining parameter approaches zero. It therefore follows that the exact SG phase distributions can always be approximated to any desired degree of accuracy by choosing the coarse-graining parameter to be suitably small. Since for any (nonzero) value of the coarse-graining parameter the well-behaved sampling functions can explicitly be calculated, the SG phase distributions can directly be sampled from the recorded data, the systematic error being determined by the coarse-graining parameter. It is worth noting that the sampling procedure can simultaneously be performed for different coarse-graining parameters, so that the systematic errors in the reconstruction of the phase distributions can easily be controlled. In practice the number of measurements is always finite and therefore statistical errors are introduced, which can also be estimated using the sampling method [13]. Hence, a suitable coarse-graining parameter is found when (for chosen number of measurement events) the systematic errors are reduced below the statistical ones. Further decrease of the coarse-graining parameter obviously makes no sense, because now the errors are fully determined by the finite sample size.

This paper is organized as follows. In Sec. II coarse-grained cosine and sine phase distributions are introduced. Section III is devoted to the relations of the phase distributions to the field-strength distributions and the calculation of the cosine and sine phase sampling functions. In Sec. IV results of computer simulations of measurements of the SG cosine and sine phase distributions for a squeezed vacuum state are presented, and error estimations are given. Finally, a summary and some concluding remarks are given in Sec. V.

II. COARSE-GRAINED COSINE AND SINE PHASE DISTRIBUTIONS

Using the exponential phase operator

$$\hat{E}=\sum_{n=0}^{\infty}|n\rangle\langle n+1| \tag{1}$$

($\hat{n}\,|n\rangle = n\,|n\rangle$, $\hat{n}=\hat{a}^{\dagger}\hat{a}$, $[\hat{a},\hat{a}^{\dagger}]=1$), Susskind and Glogower [2] introduced the Hermitian cosine and sine operators

$$\hat{C}=\tfrac{1}{2}(\hat{E}+\hat{E}^{\dagger}) \tag{2}$$

and

$$\hat{S}=-\tfrac{1}{2}i(\hat{E}-\hat{E}^{\dagger}), \tag{3}$$

respectively, which satisfy the eigenvalue equations

$$\hat{C}|\cos\phi\rangle=\cos\phi|\cos\phi\rangle \tag{4}$$

($0\leqslant\phi\leqslant\pi$) and

$$\hat{S}|\sin\phi\rangle=\sin\phi|\sin\phi\rangle \tag{5}$$

($-\pi/2\leqslant\phi\leqslant\pi/2$). The SG cosine and sine phase states $|\cos\phi\rangle$ and $|\sin\phi\rangle$, respectively, form orthonormal and complete sets in the Hilbert space, that is to say,

$$\langle\cos\phi|\cos\phi'\rangle=\delta(\phi-\phi'), \tag{6}$$

$$\int_0^{\pi}d\phi|\cos\phi\rangle\langle\cos\phi|=\hat{I}, \tag{7}$$

and

$$\langle\sin\phi|\sin\phi'\rangle=\delta(\phi-\phi'), \tag{8}$$

$$\int_{-\pi/2}^{\pi/2}d\phi|\sin\phi\rangle\langle\sin\phi|=\hat{I}. \tag{9}$$

In order to give a unified approach to the states, let us consider the ψ-parametrized Hermitian operator

$$\hat{C}(\psi)=\tfrac{1}{2}(\hat{E}e^{-i\psi}+\hat{E}^{\dagger}e^{i\psi}). \tag{10}$$

Recalling Eq. (1), $\hat{C}(\psi)$ is easily proved to satisfy the eigenvalue equation

$$\hat{C}(\psi)|\Phi,\psi\rangle=\cos\Phi|\Phi,\psi\rangle, \tag{11}$$

where

$$|\Phi,\psi\rangle=\sqrt{\frac{2}{\pi}}\sum_n e^{in\psi}\sin[(n+1)\Phi]|n\rangle. \tag{12}$$

Note that $|-\Phi,\psi\rangle=-|\Phi,\psi\rangle$ and $|\Phi+\pi,\psi\rangle=-|\Phi,\psi+\pi\rangle$. For chosen ψ the states $|\Phi,\psi\rangle$, $0\leqslant\Phi\leqslant\pi$, form an orthonormal complete basis. The SG cosine and sine phase states in Eqs. (4) and (5), respectively, can be obtained by appropriately specifying the states $|\Phi,\psi\rangle$,

$$|\cos\phi\rangle=|\Phi=\phi,\psi=0\rangle, \tag{13}$$

$$|\sin\phi\rangle=|\Phi=\tfrac{1}{2}\pi-\phi,\psi=\tfrac{1}{2}\pi\rangle. \tag{14}$$

With regard to measurements, we now introduce coarse-grained states as

$$|\Phi,\psi,\epsilon\rangle=\frac{1}{\sqrt{\epsilon}}\int_{\Phi-\epsilon/2}^{\Phi+\epsilon/2}d\Phi'|\Phi',\psi\rangle. \tag{15}$$

Using Eq. (12), the states $|\Phi,\psi,\epsilon\rangle$ can be given by

$$|\Phi,\psi,\epsilon\rangle=\sqrt{\frac{2\epsilon}{\pi}}\sum_n e^{in\psi}\sin[(n+1)\Phi]\,\mathrm{sinc}[(n+1)\epsilon/2]|n\rangle \tag{16}$$

($\mathrm{sinc}x = \sin x/x$). They are normalized to unity,

$$\langle\Phi,\psi,\epsilon|\Phi,\psi,\epsilon\rangle=1, \tag{17}$$

and tend to the exact states $|\Phi,\psi\rangle$ as ϵ approaches zero,

$$\lim_{\epsilon\to 0}\frac{1}{\sqrt{\epsilon}}|\Phi,\psi,\epsilon\rangle=|\Phi,\psi\rangle. \tag{18}$$

The coarse-grained cosine and sine phase states, respectively, are obtained as $|\cos\phi,\epsilon\rangle=|\Phi=\phi,\psi=0,\epsilon\rangle$ and $|\sin\phi,\epsilon\rangle=|\Phi=\frac{1}{2}\pi-\phi,\psi=\frac{1}{2}\pi,\ \epsilon\rangle$ [cf. Eqs. (13), (14), and (15)]. According to Eq. (18), they approach the exact SG cosine and sine phase states in the limit when $\epsilon\to 0$.

The states $|\Phi,\psi,\epsilon\rangle$ can be used to define parametrized phase distributions of a radiation-field mode via their overlaps with the quantum state $\hat{\varrho}$ of the mode

$$p(\Phi,\psi,\epsilon)=\frac{1}{\mathcal{N}(\psi,\epsilon)}\,\tilde{p}(\Phi,\psi,\epsilon) \tag{19}$$

where

$$\tilde{p}(\Phi,\psi,\epsilon)=\langle\Phi,\psi,\epsilon|\hat{\varrho}|\Phi,\psi,\epsilon\rangle, \tag{20}$$

$$\mathcal{N}(\psi,\epsilon)=\int_0^{\pi}d\Phi\,\tilde{p}(\Phi,\psi,\epsilon). \tag{21}$$

Note that $p(\Phi,\psi,\epsilon)\to p(\Phi,\psi)\equiv\langle\Phi,\psi|\hat{\varrho}|\Phi,\psi\rangle$ when $\epsilon\to 0$. In particular, the coarse-grained cosine and sine phase-state distributions $p_c(\phi,\epsilon)$ and $p_s(\phi,\epsilon)$ are given by

$$p_c(\phi,\epsilon)=p(\Phi=\phi,\psi=0,\epsilon), \tag{22}$$

$$p_s(\phi,\epsilon)=p(\Phi=\tfrac{1}{2}\pi-\phi,\psi=\tfrac{1}{2}\pi,\epsilon) \tag{23}$$

[$p_c(\phi)\equiv\langle\cos\phi|\hat{\varrho}|\cos\phi\rangle=\lim_{\epsilon\to 0}p_c(\phi,\epsilon)$, $p_s(\phi)\equiv\langle\phi|\varrho|\sin\phi\rangle=\lim_{\epsilon\to 0}p_s(\phi,\epsilon)$]. The smaller the value of ϵ becomes the better the coarse-grained distributions approximate to the exact ones. In Figs. 1 and 2 plots of $p_c(\phi,\epsilon)$ and $p_s(\phi,\epsilon)$ for various values of ϵ are shown for a mode prepared in a coherent state. We see that with an increasing value of the mean number of photons the value of ϵ must be decreased in order to obtain the coarse-grained distributions comparably close to the exact ones. This is, of course, a reflection of the fact that with a decreasing value of ϵ the value of the (effective) cutoff photon number in the expansion (16) is increased.

III. RELATIONS TO THE PHASE-PARAMETRIZED FIELD-STRENGTH DISTRIBUTIONS

When we let $\epsilon=0$, then Eq. (16) reduces, after multiplication by $\epsilon^{-1/2}$, to the expansion in the photon-number basis of the exact states $|\Phi,\psi\rangle$. All the photon-number states are seen to contribute to the exact states with comparable weight, which prevents one from explicitly calculating the

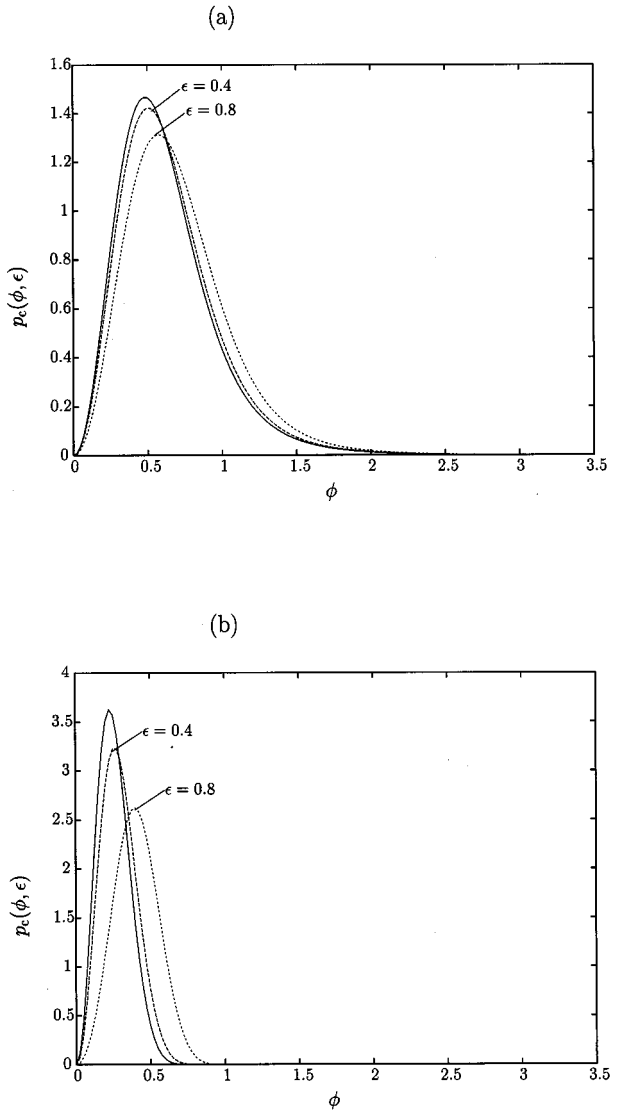

FIG. 1. The coarse-grained cosine phase state distributions of a mode prepared in a coherent state $|\alpha\rangle$ with $\langle\hat{n}\rangle=1$ ($\alpha=1$) (a) and $\langle\hat{n}\rangle=2$ ($\alpha=\sqrt{2}$) (b) are shown for $\epsilon=0.4$ (dashed lines) and $\epsilon=0.8$ (dotted lines). For comparison, the exact distributions that are observed in the limit $\epsilon\to 0$ are also shown (solid lines).

sampling functions for the exact SG phase distributions. The advantage of the coarse-grained distributions is that the sampling functions can be calculated in a straightforward way. They are well behaved, so that the phase distributions can be directly sampled from the recorded data. Since for sufficiently small values of the coarse-graining parameter the systematic errors that arise from it can be reduced below any desired level, the method enables one to measure the exact distributions with accuracies that are only determined by the statistical errors due to the finite number of sampling points.

The difference-photocurrent statistics recorded in balanced homodyning represents the statistics of a scaled field strength (quadrature component) of the signal mode,

$$\hat{F}(\varphi)=|F|(\hat{a}e^{-i\varphi}+\hat{a}^{\dagger}e^{i\varphi}), \tag{24}$$

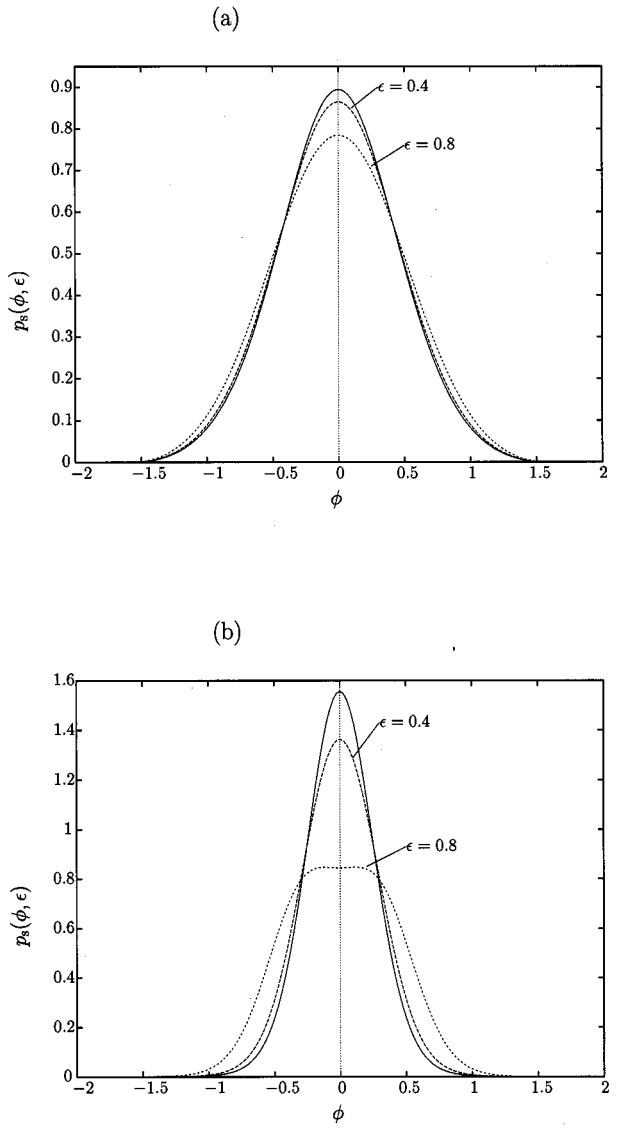

FIG. 2. The coarse-grained sine phase state distributions of a mode prepared in a coherent state $|\alpha\rangle$ with $\langle\hat{n}\rangle=1$ ($\alpha=1$) (a) and $\langle\hat{n}\rangle=2$ ($\alpha=\sqrt{2}$) (b) are shown for $\epsilon=0.4$ (dashed lines) and $\epsilon=0.8$ (dotted lines). For comparison, the exact distributions that are observed in the limit $\epsilon\rightarrow 0$ are also shown (solid lines).

where the phase φ is determined by the chosen phase parameters of the apparatus (see, e.g., [14]). The desired sampling functions can therefore be obtained from the integral relations between the coarse-grained phase distributions $p(\Phi,\psi,\epsilon)$ and the phase-parametrized field-strength distributions of the signal field,

$$p(\mathcal{F},\varphi)=\langle\mathcal{F},\varphi|\hat{\varrho}|\mathcal{F},\varphi\rangle, \tag{25}$$

$|\mathcal{F},\varphi\rangle$ being the eigenvectors of $\hat{F}(\varphi)$ (for details, see [14,15]). For this purpose the density operator $\hat{\varrho}$ is expanded as [16,17,6]

$$\hat{\varrho}=\int_0^{\pi} d\varphi \int_{-\infty}^{\infty} d\mathcal{F}\, p(\mathcal{F},\varphi;s)\hat{K}(\mathcal{F},\varphi;-s), \tag{26}$$

where the smeared field-strength distributions $p(\mathcal{F},\varphi;s)$, $s=1-\eta^{-1}$, have been introduced, which are measured in nonperfect detection, i.e., when the detection efficiency η is less than unity (see, e.g., [14]). The operator integral kernel $\hat{K}(\mathcal{F},\varphi;-s)$ in Eq. (26) is given by

$$\hat{K}(\mathcal{F},\varphi;-s)=\frac{|F|^2}{\pi}\int_{-\infty}^{\infty} dy|y| \times\exp\{iy[\hat{F}(\varphi)-\mathcal{F}]-\tfrac{1}{2}sy^2|F|^2\}. \tag{27}$$

Using Eq. (26), from Eq. (20) we easily find that $\tilde{p}(\Phi,\psi,\epsilon)$ can be related to $p(\mathcal{F},\varphi;s)$ as

$$\tilde{p}(\Phi,\psi,\epsilon)=\int_0^{\pi} d\varphi\int_{-\infty}^{\infty} d\mathcal{F}\, p(\mathcal{F},\varphi;s)K_\epsilon(\Phi,\psi,\mathcal{F},\varphi;s), \tag{28}$$

where

$$K_\epsilon(\Phi,\psi,\mathcal{F},\varphi;s)=\langle\Phi,\psi,\epsilon|\hat{K}(\mathcal{F},\varphi;-s)|\Phi,\psi,\epsilon\rangle. \tag{29}$$

Equation (28) can be regarded as the basic equation for direct sampling of the phase distributions $p(\Phi,\psi,\epsilon)$ from the difference-photocurrent statistics in balanced homodyning, where the integral kernel play the role of the sampling function. In order to calculate it, we substitute in Eq. (29) for $|\Phi,\psi,\epsilon\rangle$ the expansion Eq. (16) and derive

$$K_\epsilon(\Phi,\psi,\mathcal{F},\varphi;s)=\frac{2\epsilon}{\pi}\sum_{n=0}^{\infty}\sum_{m=0}^{\infty}\{f_{nm}(x;s)\exp[i(n-m) \times(\varphi-\psi)]\sin[(n+1)\Phi] \times\sin[(m+1)\Phi]\mathrm{sinc}[(n+1)\epsilon/2] \times\mathrm{sinc}[(m+1)\epsilon/2]\}, \tag{30}$$

where the function $f_{nm}(x;s)$, $x=\mathcal{F}/(\sqrt{2}|F|)$, is closely related to the sampling function

$$\langle n|\hat{K}(\mathcal{F},\varphi;-s)|m\rangle=f_{nm}(x;s)\exp[i(n-m)\varphi] \tag{31}$$

for measuring the signal-mode density matrix in the photon-number basis [6]. From inspection of Eqs. (27) and (30) we see that the symmetry relations

$$K_\epsilon(\Phi,\psi,\mathcal{F},\varphi+\pi;s)=K_\epsilon(\Phi,\psi,-\mathcal{F},\varphi;s), \tag{32}$$

$$K_\epsilon(\Phi,\psi,\mathcal{F},\varphi+\pi;s)=K_\epsilon(\Phi-\pi,\psi,\mathcal{F},\varphi;s), \tag{33}$$

$$K_\epsilon(-\Phi,\psi,\mathcal{F},\varphi;s)=K_\epsilon(\Phi,\psi,\mathcal{F},\varphi;s), \tag{34}$$

$$K_\epsilon(\Phi,-\psi,\mathcal{F},-\varphi;s)=K_\epsilon(\Phi,\psi,\mathcal{F},\varphi;s), \tag{35}$$

$$K_\epsilon(\Phi,\psi,\mathcal{F},\varphi;s)=K_\epsilon(\Phi,0,\mathcal{F},\varphi-\psi;s) \tag{36}$$

are valid. Hence knowing the function

$$K_\epsilon(\Phi,\mathcal{F},\varphi;s)\equiv K_\epsilon(\Phi,\psi=0,\mathcal{F},\varphi;s), \tag{37}$$

with $\Phi,\varphi\in(\pi/2)$ intervals, the function $K_\epsilon(\Phi,\psi,\mathcal{F},\varphi;s)$ is known for all values of Φ, ψ, and φ. In particular, the functions $K_\epsilon^c(\phi,\mathcal{F},\varphi;s)$ and $K_\epsilon^s(\phi,\mathcal{F},\varphi;s)$, respectively, that are

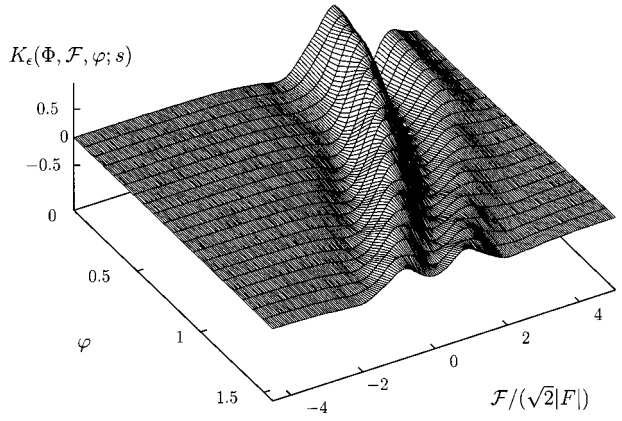

FIG. 3. The dependence on $\mathcal{F}$ and φ of the sampling function $K_\epsilon(\Phi,\mathcal{F},\varphi;s)$ is shown for $\Phi=\frac{1}{8}\pi$, the values of s and ϵ being $s=0$ (perfect detection) and $\epsilon=0.4$.

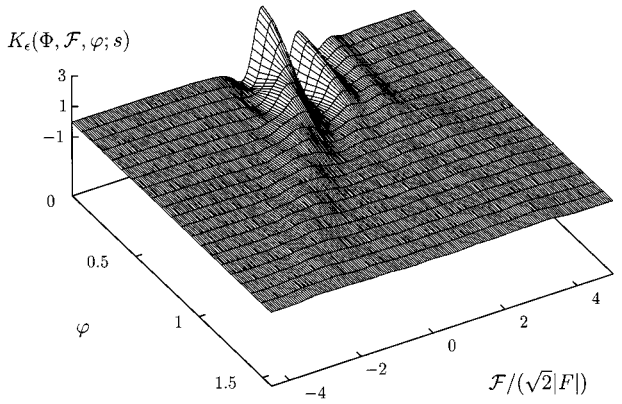

FIG. 5. The dependence on $\mathcal{F}$ and φ of the sampling function $K_\epsilon(\Phi,\mathcal{F},\varphi;s)$ is shown for $\Phi=\frac{3}{8}\pi$, the values of s and ϵ being $s=0$ (perfect detection) and $\epsilon=0.4$.

required in order to relate the cosine and sine phase states distributions $p_c(\phi,\epsilon)$ and $p_s(\phi,\epsilon)$ to the field-strength distributions are given by

$$K_\epsilon^c(\phi,\mathcal{F},\varphi;s)=K_\epsilon(\Phi=\phi,\mathcal{F},\varphi;s), \tag{38}$$

$$K_\epsilon^s(\phi,\mathcal{F},\varphi;s)=K_\epsilon(\Phi=\phi-\tfrac{1}{2}\pi,\mathcal{F},\varphi-\tfrac{1}{2}\pi;s). \tag{39}$$

The function $f_{nm}(x;s)$ in the series expansion (30) of the sampling function $K_\epsilon(\Phi,\mathcal{F},\varphi;s)$, Eq. (37), has been studied in a number of papers and different algorithms for numerical calculations have been discussed (see [13,18] and references therein). For the sake of transparency let us restrict our attention to perfect detection ($\eta=1$ and hence $s=1-\eta^{-1}=0$). In this case, $f_{nm}(x)\equiv f_{nm}(x,s=0)$ can be written as

$$f_{nm}(x)=\frac{d}{dx}[\psi_n(x)\phi_m(x)] \quad \text{if } m\geqslant n \tag{40}$$

$[f_{nm}(x)=f_{mn}(x)$ if $m<n]$, where $\psi_n(x)$ and $\phi_m(x)$, respectively, are the regular (normalizable) and irregular (unnormalizable) solutions of the energy eigenvalue equation of the harmonic oscillator for the nth eigenvalue [18,13]. The asymptotic behavior of $f_{nm}(x)$ for large values of n and m can be found using the semiclassical (WKB) approximation. For the argument x within the classical allowed region $|x|<a_n\equiv(2n+1)^{1/2}$ the function $f_{nm}(x)$ $(m\geqslant n)$ becomes [13]

$$f_{nm}(x)\sim\frac{2}{\pi}(p_np_m)^{-1/2}[p_m\cos(S_n+\tfrac{1}{4}\pi)\cos(S_m+\tfrac{1}{4}\pi) - p_n\sin(S_n+\tfrac{1}{4}\pi)\sin(S_m+\tfrac{1}{4}\pi)], \tag{41}$$

where

$$p_n(x)=(2n+1-x^2)^{1/2} \tag{42}$$

denotes the classical momentum and

$$S_n(x)=\int_{a_n}^{x}dx'\,p_n(x') \tag{43}$$

is the time-independent part of the classical action.

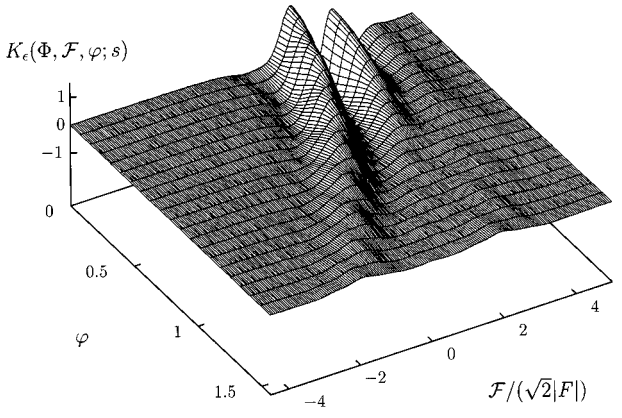

FIG. 4. The dependence on $\mathcal{F}$ and φ of the sampling function $K_\epsilon(\Phi,\mathcal{F},\varphi;s)$ is shown for $\Phi=\frac{1}{4}\pi$, the values of s and ϵ being $s=0$ (perfect detection) and $\epsilon=0.4$.

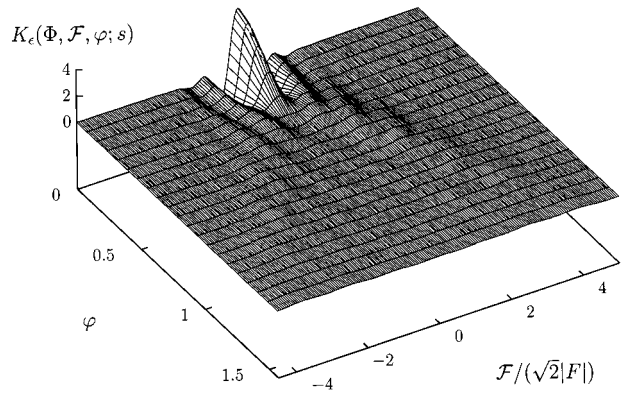

FIG. 6. The dependence on $\mathcal{F}$ and φ of the sampling function $K_\epsilon(\Phi,\mathcal{F},\varphi;s)$ is shown for $\Phi=\frac{1}{2}\pi$, the values of s and ϵ being $s=0$ (perfect detection) and $\epsilon=0.4$.

For proving the convergence of the series expansion of $K_\epsilon(\Phi,\mathcal{F},\varphi;s=0)$, it is sufficient to substitute in Eq. (30) for $f_{nm}(x;s=0)$ the semiclassical expression (41). For $x/a_n\rightarrow 0$ the functions $p_n(x)$ and $S_n(x)$ in Eq. (41) behave like $n^{1/2}$ and $-(n+\frac{1}{2})\pi/2$, respectively, so that $[p_m(x)/p_n(x)]^{1/2}\sim(m/n)^{1/4}$ and $\cos[S_n(x)+\pi/4]\sim\cos(n\pi/2)$, $\sin[S_n(x)+\pi/4]\sim-\sin(n\pi/2)$. Hence for any $\epsilon>0$ the series expansion is expected to exist, because of the factor $(nm)^{-1}$ that arises from the sinc functions. Results of numerical calculations of $K_\epsilon(\Phi,\mathcal{F},\varphi;s=0)$ are shown in Figs. 3–6. It should be noted that $K_\epsilon(\Phi,\mathcal{F},\varphi;s)$ separately depends on the two phases Φ and φ, whereas the sampling function for the London phase state distribution only depends on the difference phase [12].

IV. DIRECT SAMPLING OF THE SG PHASE DISTRIBUTIONS

In order to demonstrate the feasibility of direct sampling of the SG cosine and sine phase state distributions from the recorded difference-photocurrent statistics in balanced homodyning, we have performed computer simulations of measurements of the phase-parametrized field-strength distributions $p(\mathcal{F},\varphi)$ on an equidistant grid of points $\{\mathcal{F}_i,\varphi_j\}$ (for simplicity, the discrete intervals $\Delta\varphi$ and $\Delta\mathcal{F}$ in the experiment are considered as differentials). We have assumed that in the experiments the signal mode to be detected is prepared in a squeezed vacuum state

$$|\Psi\rangle=\exp\{-\tfrac{1}{2}[\xi(\hat{a}^\dagger)^2-\xi^*\hat{a}^2]\}|0\rangle. \tag{44}$$

Before presenting results, let us address the problem of errors. For estimating the statistical errors that are unavoidably connected with the finite sample size in any realistic experiment, we follow the arguments given in [13] and assume that homodyne detection is a Poissonian process for statistically independent $\mathcal{F}$ values at phases φ. The experimentally measured distributions $p_{\rm est}(\mathcal{F},\varphi;s)$ are estimates of the exact distributions $p(\mathcal{F},\varphi;s)$, and the use of $p_{\rm est}(\mathcal{F},\varphi;s)$ in the sampling formula (28) then yields estimates $\widetilde{p}_{\rm est}(\Phi,\psi,\epsilon)$ of $\widetilde{p}(\Phi,\psi,\epsilon)$. Thus the variance $\sigma^2_{\widetilde{p}_{\rm est}}(\Phi,\psi,\epsilon)$ may be estimated as

$$\sigma^2_{\widetilde{p}_{\rm est}}(\Phi,\psi,\epsilon)\approx\int_0^\pi\frac{d\varphi}{N(\varphi)}\int_{-\infty}^{\infty}d\mathcal{F}\,p_{\rm est}(\mathcal{F},\varphi;s)\times K_\epsilon^2(\Phi,\psi,\mathcal{F},\varphi;s), \tag{45}$$

where $N(\varphi)$ is the number of samples per phase interval at phase φ. Equation (45) reveals that the estimation of the statistical errors can also be performed in *real time*. Using Eq. (45), the variance of the normalization factor $\mathcal{N}_{\rm est}$ [obtained according to Eq. (21), with $\widetilde{p}_{\rm est}(\Phi,\psi,\epsilon)$ in place of $\widetilde{p}(\Phi,\psi,\epsilon)$] may then be estimated as

$$\sigma^2_{\mathcal{N}_{\rm est}}(\psi,\epsilon)\approx\int_0^\pi\frac{d\varphi}{N(\varphi)}\int_{-\infty}^{\infty}d\mathcal{F}\,p_{\rm est}(\mathcal{F},\varphi;s)\overline{K^2_\epsilon}(\mathcal{F};s), \tag{46}$$

where

$$\overline{K_\epsilon}(\mathcal{F};s)=\int_0^\pi d\Phi K_\epsilon(\Phi,\psi,\mathcal{F},\varphi;s)=2\epsilon\sum_{n=0}^{\infty}f_{nn}(x;s)\,\mathrm{sinc}^2[(n+1)\epsilon/2] \tag{47}$$

[cf. Eq. (30)]. Note that $K_\epsilon(\Phi,\psi,\mathcal{F},\varphi;s)$ and $\overline{K_\epsilon}(\mathcal{F};s)$ differ in the contributions of the off-diagonal elements $\langle n|\hat{K}(\mathcal{F},\varphi;-s)|m\rangle$, $n\neq m$. The variance of the estimated phase distribution $p_{\rm est}(\Phi,\psi,\epsilon)=\widetilde{p}_{\rm est}(\Phi,\psi,\epsilon)/\mathcal{N}_{\rm est}(\psi,\epsilon)$ can eventually be estimated as (see, e.g., [19])

$$\sigma^2_{p_{\rm est}}(\Phi,\psi,\epsilon)\approx p^2_{\rm est}(\Phi,\psi,\epsilon)\left[\frac{\sigma^2_{\widetilde{p}_{\rm est}}(\Phi,\psi,\epsilon)}{\widetilde{p}^2_{\rm est}(\Phi,\psi,\epsilon)}+\frac{\sigma^2_{\mathcal{N}_{\rm est}}(\psi,\epsilon)}{\mathcal{N}^2_{\rm est}(\psi,\epsilon)}-2\frac{\kappa_{\widetilde{p}_{\rm est}\mathcal{N}_{\rm est}}(\Phi,\psi,\epsilon)}{\widetilde{p}_{\rm est}(\Phi,\psi,\epsilon)\mathcal{N}_{\rm est}(\psi,\epsilon)}\right], \tag{48}$$

where

$$\kappa_{\widetilde{p}_{\rm est}\mathcal{N}_{\rm est}}(\Phi,\psi,\epsilon)\approx\int_0^\pi\left[\frac{d\varphi}{N(\varphi)}\times\int_{-\infty}^{\infty}d\mathcal{F}\,p_{\rm est}(\mathcal{F},\varphi;s)\times K_\epsilon(\Phi,\psi,\mathcal{F},\varphi;s)\overline{K_\epsilon}(\mathcal{F};s)\right] \tag{49}$$

is the correlation between the unnormalized distribution and the normalization factor.

To give a quantitative measure of the systematic errors arising from the nonvanishing coarse-graining parameter, let us consider the factor

$$\mathcal{Q}(\psi,\epsilon)=\epsilon^{-1}\mathcal{N}(\psi,\epsilon), \tag{50}$$

which has the property that [cf. Eqs. (17), (20), and (21)]

$$\lim_{\epsilon\rightarrow 0}\mathcal{Q}(\psi,\epsilon)=\lim_{\epsilon\rightarrow 0}\sum_{n=0}^{\infty}\mathrm{sinc}^2[(n+1)\epsilon/2]\langle n|\hat{\varrho}|n\rangle=1 \tag{51}$$

for any physical quantum state $\hat{\varrho}$. The measured estimates $\mathcal{Q}_{\rm est}(\psi,\epsilon)$ and $\sigma^2_{\mathcal{Q}_{\rm est}}(\psi,\epsilon)=\epsilon^{-2}\sigma^2_{\mathcal{N}_{\rm est}}(\psi,\epsilon)$ can then be used to obtain a criterion of choosing a suitable value of the coarse-graining parameter ϵ. Different values of ϵ give rise to different sampling functions $K_\epsilon(\Phi,\psi,\mathcal{F},\varphi;s)$. Starting with a (small) value of ϵ, the measured data can be sampled simultaneously for different, decreasing values of ϵ. In this way the systematic errors can be reduced such that $\mathcal{Q}_{\rm est}(\psi,\epsilon)\sim 1$ within the root-mean-square deviation $\sigma_{\mathcal{Q}_{\rm est}}(\psi,\epsilon)$. The errors are then given by the statistical ones, and further decrease of ϵ does not improve the accuracy of the sampled distributions. Clearly, when the number of sampling points is increased, so that the statistical errors are decreased, then ϵ must also be decreased in order to ensure that the systematic errors are below the statistical ones.

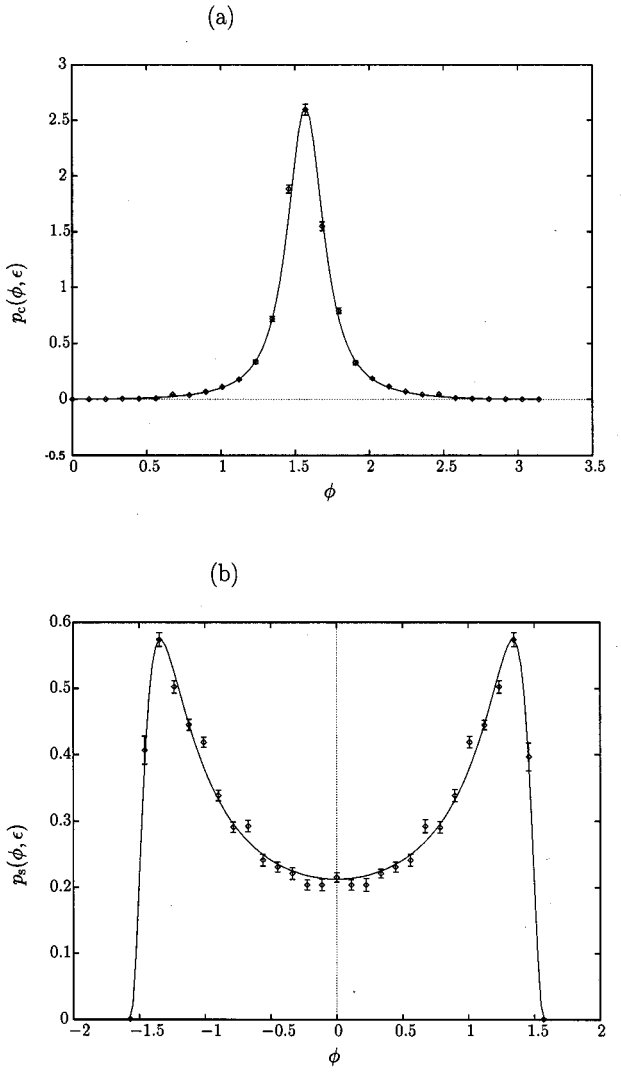

FIG. 7. The sampled Susskind-Glogower cosine (a) and sine (b) phase state distributions (points with error bars) of a signal mode prepared in a squeezed vacuum state, Eq. (44), with mean photon number $\langle\hat{n}\rangle=1$ ($\xi=0.88$) are shown and compared with the calculated distributions (full lines), the values of s and ϵ being $s=0$ (perfect detection) and $\epsilon=0.1$. In the computer simulation of the measurements 30 phases have been considered and 10^3 events have been assumed to be recorded at each phase. The error bars indicate the root-mean-square deviations according to Eq. (48).

In our computer experiments we have assumed that measurements at 30 phases are performed and 10^3 events at each phase are recorded (cf. Ref. [4]). From the results shown in Fig. 7 we see that the measured SG phase distributions are in good agreement with the theoretical predictions. The error bars indicate the standard deviations obtained according to Eq. (48). The value of ϵ has been determined from the measured data as outlined above. The systematic errors have been found to reduce below the statistical ones when $\epsilon\leqslant 10^{-1}$. From Eqs. (12) [together with Eqs. (13) and (14)] and (44) we easily see that the cosine and sine phase distributions of the ordinary vacuum ($\xi=0$) are given by $|\langle 0|\cos\phi\rangle|^2=(2/\pi)\sin^2\phi$ and $|\langle 0|\sin\phi\rangle|^2=(2\pi)^{-1}\cos^2\phi$, respectively. In this case the cosine phase state distribution has a broad maximum at $\phi=\pi/2$, whereas the sine phase state distribution has a broad maximum at $\phi=0$. When the value of ξ is increased ($\xi>0$), the ''vacuum noise circle'' centered at the origin of coordinates in the (complex) α phase space is squeezed to an ellipse with the small semiaxis parallel to the real axis [20]. Hence, the cosine phase distribution is expected to become more sharply peaked at $\phi=\pi/2$. Accordingly, the sine phase state distribution is expected to show a double-peak structure, with the maxima close to $\phi=\pm\pi/2$ and the minimum at $\phi=0$.

V. SUMMARY AND CONCLUSIONS

In this paper we have studied the problem of measuring the SG cosine and sine phase state distributions in balanced homodyne detection. For this purpose we have introduced coarse grained cosine and sine phase distributions such that they always approximate to the exact SG cosine and sine phase distributions to any desired degree of accuracy, if the coarse-graining parameter is suitably small.

We have shown that the coarse-grained phase distributions can be directly sampled from the recorded difference-photocurrent statistics. The direct sampling method has a number of advantages over indirect methods, such as reconstruction of the Wigner function from smoothed experimental data and calculation of the phase statistics from the reconstructed Wigner function. In particular, the sampling method is fast and the phase distributions can be obtained in *real time*, without storage of large amounts of data. Further, the sampling method also enables one to estimate the statistical errors introduced by the finite sample size.

For chosen sample size the systematic errors resulting from coarse-graining can be reduced below the statistical errors, provided that the coarse-graining parameter is suitably small. In this way, the SG phase distributions can always be measured with an accuracy determined by the statistical errors. The coarse-graining parameter can be obtained either from some *a priori* information about the state or from the sampling method. Performing the sampling procedure for different, decreasing coarse-graining parameters simultaneously, a suitable coarse-graining parameter is found when further decrease of the parameter does not change the errors.

It is worth noting that the SG cosine and sine phase state distributions can be regarded as special cases of ψ-parametrized phase state distributions. The latter are based on ψ-parametrized phase states that for $\psi=0$ and $\psi=\frac{1}{2}\pi$ reduce to the cosine and sine phase states, respectively. Accordingly, the sampling functions for the cosine and sine phase state distributions can be obtained by specifying the sampling function for the ψ-parametrized phase distributions. Their integral relation to the field-strength distributions reveals that the sampling function exhibits a number of symmetry properties that can be used advantageously in calculations.

We have calculated the sampling function using an expansion in terms of the matrix elements of the corresponding operator integral kernel in the Fock basis. These matrix elements, which are the sampling functions required for measuring the signal-mode density matrix in the Fock basis, can be calculated applying the algorithm developed in [13]. In this way, the sampling function can be obtained for any

(nonzero) coarse-graining parameter.

In order to give an example, we have performed computer simulations of measurements of the SG cosine and sine phase state distributions for a realistic grid of sampling points and estimated the errors. Assuming that the signal mode is prepared in a squeezed vacuum state, the measured phase distributions have been found to reproduce the exact ones with sufficiently high precision. The definite value of the coarse-graining parameter has been found reconstructing the phase distributions for different probe values.

It is worth noting that the different shaping of the cosine and sine phase distributions demonstrates the quantum character of the state of the signal mode. They reflect the fact that for quantum states the (noncommuting) cosine and sine quantities cannot be related to a common phase. This effect is of course not observed in the London phase distribution that is related to a non-Hermitian operator.

ACKNOWLEDGMENTS

This work was supported by the Deutsche Forschungsgemeinschaft. We would like to thank T. Opatrný and U. Leonhardt for discussions.

[1] R. Lynch, Phys. Rep. **256**, 367 (1995).
[2] L. Susskind and J. Glogower, Physics **1**, 49 (1964); P. Carruthers and M.M. Nieto, Phys. Rev. Lett. **14**, 387 (1965); Rev. Mod. Phys. **40**, 411 (1968).
[3] J.W. Noh, A. Fougères, and L. Mandel, Phys. Rev. Lett. **67**, 1426 (1991); **71**, 2579 (1993); Phys. Rev. A **45**, 424 (1992); **46**, 2840 (1992); **47**, 4535 (1993); **47**, 4541 (1993).
[4] D.T. Smithey, M. Beck, A. Faridani, and M.G. Raymer, Phys. Rev. Lett. **70**, 1244 (1993); D.T. Smithey, M. Beck, J. Cooper, M.G. Raymer, and A. Faridani, Phys. Scr. **T48**, 35 (1993).
[5] G. Breitenbach, T. Müller, S.F. Pereira, J.-Ph. Poizat, S. Schiller, and J. Mlynek, J. Opt. Soc. Am. B **12**, 2304 (1995).
[6] G.M. D'Ariano, C. Macchiavello, and M.G.A. Paris, Phys. Rev. A **50**, 4298 (1994); G.M. D'Ariano, Quantum Semiclass. Opt. **7**, 693 (1995); G.M. D'Ariano, U. Leonhardt, and H. Paul, Phys. Rev. A **52**, R1801 (1995); U. Leonhardt, H. Paul, and G.M. D'Ariano, *ibid.* **52**, R1801 (1995); H. Kühn, D.-G. Welsch, and W. Vogel, J. Mod. Opt. **41**, 1607 (1994); A. Zucchetti, W. Vogel, M. Tasche, and D.-G. Welsch, Phys. Rev. A **54**, 1678 (1996).
[7] S. Schiller, G. Breitenbach, S.F. Pereira, T. Müller, and J. Mlynek, Phys. Rev. Lett. **77**, 2933 (1996).
[8] M. Munroe, D. Boggavarapu, M.E. Anderson, and M.G. Raymer, Phys. Rev. A **52**, R924 (1995).
[9] T. Opatrný, D.-G. Welsch, and W. Vogel, Phys. Rev. A (to be published); Opt. Commun. (to be published); Proceedings of the 4th Central European Workshop on Quantum Optics, Budmerice, 1996 [Acta Phys. Slov. **46**, 469 (1996)]; M.G. Raymer, D.F. McAlister, and U. Leonhardt, Phys. Rev. A **54**, 2397 (1996).
[10] D.F. McAlister and M.G. Raymer (unpublished).
[11] M. Beck, D.T. Smithey, and M.G. Raymer, Phys. Rev. A **48**, R890 (1993); D.T. Smithey, M. Beck, J. Cooper, and M.G. Raymer, Phys. Rev. A **48**, 3159 (1993).
[12] M. Dakna, L. Knöll, and D.-G. Welsch, Proceedings of the 4th Central European Workshop on Quantum Optics, Budmerice, 1996 [Acta Phys. Slov. **46**, 349 (1996)].
[13] U. Leonhardt, M. Munroe, T. Kiss, M.G. Raymer, and Th. Richter, Opt. Commun. **127**, 144 (1996).
[14] W. Vogel and D.-G. Welsch, *Lectures on Quantum Optics* (Akademie-Verlag, Berlin, 1994).
[15] M. Schubert and W. Vogel, Phys. Lett. **68**A, 321 (1978).
[16] K.E. Cahill and R. Glauber, Phys. Rev. **177**, 1857 (1969).
[17] K. Vogel and H. Risken, Phys. Rev. A **40**, 2847 (1989).
[18] Th. Richter, Phys. Lett. **211**A, 327 (1996).
[19] Ph.R. Bevington, *Data Reduction and Error Analysis for the Physical Sciences* (McGraw-Hill, New York, 1969).
[20] R. Loudon and P.L. Knight, J. Mod. Opt. **34**, 709 (1987).